Chromian Spinel from Dunites of the Inagli Massif and Their Oxygen Thermobarometry (Aldan Shield, Siberian Platform)

Alexander Okrugin[1*)]

[1*)] Diamond and Precious Metal Geology Institute, Siberian Branch, Russian Academy of Sciences (DPMGI SB RAS), 39 Lenin Str, Yakutsk, 677980, Russia; okrugin@diamond.ysn.ru; https://orcid.org/0000-0002-1248-8993

http://doi.org/10.29227/IM-2024-01-16

Submission date: *2.5.2023* | Review date: *5.6.2023*

Abstract

The Inagli dunite-peridotite-shonkinite zonal-ring intrusive with platinum-chromite mineralization is located on the Aldan shield of the Siberian Platform. Considering the structure, rock composition and ore mineralization, it is similar to the platinum-bearing zonal massifs of the "Ural-Alaskan" type, but this intrusive differs from the latter in its geological position. In order to clarify the physical and chemical conditions of formation of the Inagli massif, the mineral composition of rocks, especially chromite-containing dunites, peridotites and shonkinites, as well as platinum-chromitite ore segregations, has been studied in detail. The rocks of the Inagli massif, from dunites to shonkinites, including peridotites, clinopyroxenites, and alkaline syenites, form a single continuous series. This is confirmed by a clear dependence of the composition of olivine, pyroxene, phlogopite and chromian spinel on the content of MgO in rocks. They were formed from the initial high-potassium picrite melt, which, during rising, underwent gradual decompression solidification and formed a cylindrical diapir-like body at the near-surface level in the Early Cretaceous. This occurred as a result of subduction processes related to the formation of the Mongol-Okhotsk orogenic belt along the southern framing of the Siberian craton. The values of oxygen volatility ($lgfO_2$) for dunites, peridotites, shonkinites, chromitites and olivine-chromite inclusions in the isoferroplatinum of the Inagli massif, calculated using the method of the olivine-spinel oxygen thermobarometer of Ballhaus-Berry-Green (BBG), form a single trend FMQ+(2-4) in the range 620-1140^{0}C, i.e. along the band by 2-4 units of $lgfO_2$ exceeding the fayalite-magnetite-quartz (FMQ) buffer. Such a rather narrow range of variation in the values of O_2 fugacity in a wide interval of temperature indicates good comparability and reliability of the data obtained. At the same time, there is a natural decrease in temperature intervals for the formation of olivine-chromite parageneses (in ^{0}C): with isoferroplatinum – (1140-680); in chromitite segregations – (980-710); in dunites – (930-620); peridotites – (890-770) and shonkinites – (840-710). The results obtained almost completely coincide with the field of values for dunites and chromitites from the Platinum-bearing belt of the Urals, given by other researchers. In terms of redox parameters, platinum-bearing zonal ultramafic-mafic massifs of the Ural-Alaskan and Aldanian types are close to more oxidized peridotites with a long history in the lithosphere. They differ significantly from the peridotites of the Beni-Bousera massif, as well as abyssal peridotites of the oceanic ridge systems, and others, which are formed under more reduced conditions corresponding to the range between FMQ, carbon-oxygen-CO (CCO) and iron-wustite (IW) buffers.

Keywords: chromian spinel, dunites of the inagli massif, oxygen thermobarometry, siberian platform

Introduction

The Inagli massif is a concentric-zonal ring intrusive consisting of a dunite core and platinum-chromite mineralization, which forms a platinum-bearing placer [1, 2]. The features of platinum group minerals (PGM) are discussed by the author in a separate article; this work focuses on the deep conditions of the primary magma development that formed the Inagli massif with the application of the olivine-spinel oxygen thermobarometer of Ballhaus-Berry-Green (BBG) [3]. This is possible due to the fact that dunites contain accessory chromite grains in the form of inclusions in olivine, as well as disseminated and massive segregations of chromitites. In addition, in placers and dunites of the Inagli massif, close intergrowths of PGM with chromite and olivine occur, wherein the mineral compositions correlate well with alterations in the magnesia value of the host rocks, which indicate the crystallization differentiation of magma [4].

The mechanism and sequence of formation of concentric-zonal rocks of the Inagli intrusive has different interpretations among researchers. In case the age of intrusion of alkaline gabbroids and syenites, according to many authors, was determined reliably as Jurassic-Cretaceous, the time of formation of the dunite core was previously considered to be Precambrian. Many researchers explain the discrete zoning of the massif, expressed as a drastic change of dunite–peridotite–pyroxenite–shonkinite rocks, by different types of metasomatic impact of alkaline basaltic melt on earlier consolidated dunites [e.g. 2]. The author proposed an alternative hypothesis of magma segregation through thermal diffusion, convection, and cumulation to explain the formation of zonal massifs of discrete mafic–ultramafic composition [5].

Geology of the Inagly massif

The Inagli massif, characterized by a circular shape with a 4,5×5,0 km in size and a concentric-zonal structure, cuts through the rocks of the Archean crystalline basement in a diapir-like shape in the intersection zone of the NW (Yukhta) and NE (Inagli) regional faults ‘Figure 1’. Syenite porphyries are formed around the massif, lying in the form of sills in the Vendian-Cambrian strata. The latter horizontally overlap the Archean metamorphic complexes with angular unconformity.

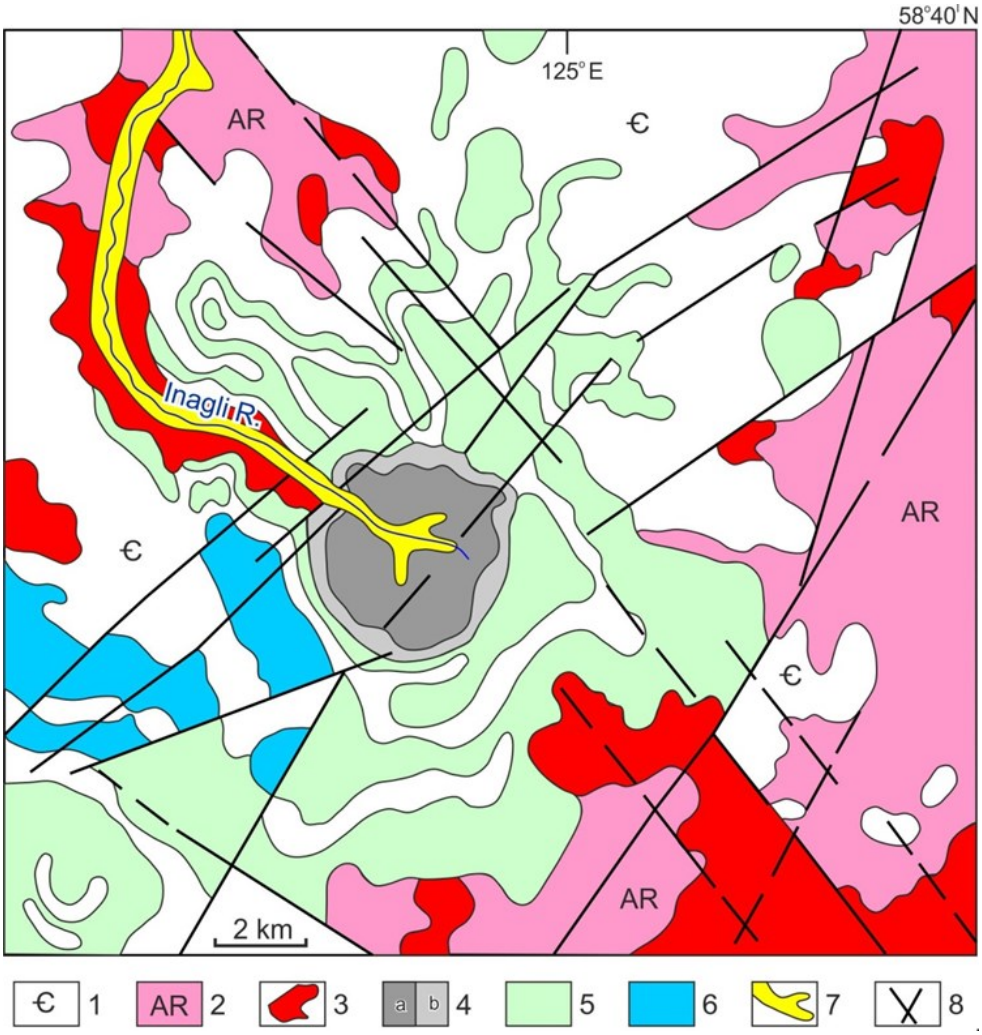

Fig. 1. Schematic geological map of the location of the Inagli massif.
1, Cambrian limestones, dolomites, sandstones and gritstones; 2, Archean rocks of the crystalline basement; 3, Archean granites; 4, dunites, peridotites and pyroxenites (a), and shonkinites (b) of the Inagli massif; 5, Early Cretaceous syenite-porphyry; 6, Jurassic syenite–diorite–porphyrites; 7, platinum placer in the Inagly R.; 8, faults. The map slightly modified after [2].

Based on geophysical data, this intrusive is identified with an object of regular cylindrical shape with a diameter of 5 km, extending to a depth of 5 km. This body is interpreted as a continuation of a flattened-expanded local anomaly, which can be identified with the expansion of the massif, i.e. with the presence of a deep magma chamber [6]. Geological and morphological characteristics of the intrusive structure demonstrate that the picrite melt which formed the Inagli massif underwent decompression solidification during the ascent, with intrusion of magma at the subsurface level in the form of a viscous diapir-like body of cylindrical shape. Based on obtained U-Pb ages of zircons from dunites (134 Ma), pyroxenites (123-126 Ma) and syenites (128 Ma), the formation time of the Inagli massif is defined as Early Cretaceous [4]. This is confirmed by the direct dating of the new ^{190}Pt-^{4}He method for isoferroplatinum (125-135 Ma) [7] and sperrylite (131-137 Ma) [8] from the Inagli plaser ‘Figure 2’.

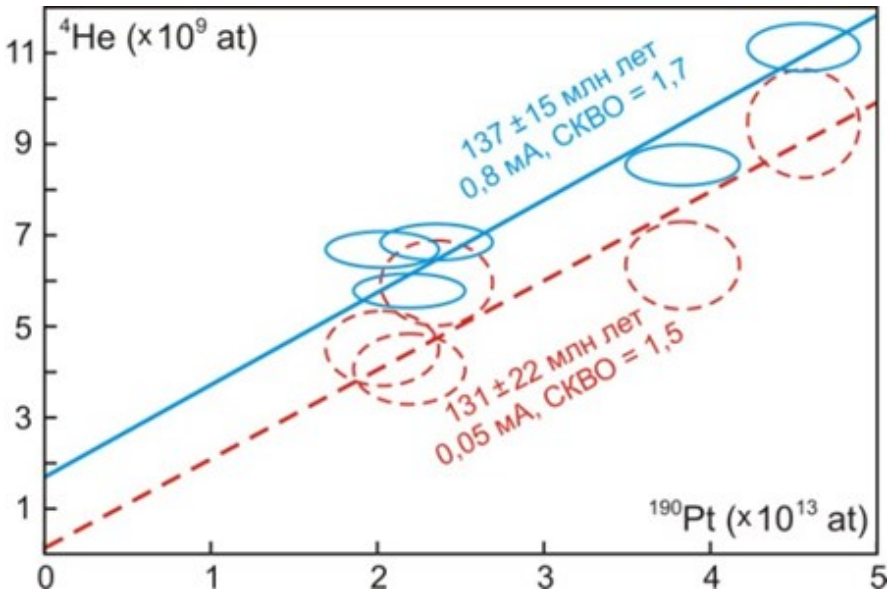

Fig. 2. ^{190}Pt-^{4}He isochron for sperrylite samples from the Inagli massif placer.

Mineral and Geochemical Compositions of the Inagli Massif Rocks

The central part of the intrusive is composed of a dunite core bordered by a margin of potassium alkaline gabbroids (mainly shonkinites) with a thickness of up to 0.5 km. Between the dunites and shonkinites there is a narrow intermittent fringe (up to 50 m), composed of peridotites and pyroxenites. Between these rocks there are no secant contacts with chilled margins or sharp mineral transformations. They pass into each other within a narrow band of rapid changes in the quantitative composition of minerals. Rocks of the Inagli massif, from dunites to pulaskites, including peridotites, clinopyroxenites, shonkinites and melanocratic alkaline syenites, form a single continuous comagmatic series. This is confirmed by a clear dependence of the compositions of olivine, pyroxene, phlogopites, and Cr-spinels on the MgO content of the rocks and on the behavior of trace elements in them. This indicates the evolutionary crystallization path of the formation of all rocks of this massif from the primary high-K picritoid melt [5].

To identify the composition of the initial melt from which the rocks of the Inagli massif were formed, the author used [4] data on the compositions of Mesozoic K-picritoids that occur in the form of sills among the Jurassic sandstones of the Yakokut graben of the Central Aldan district [9]. Mineral and geochemical characteristics show that the sill rocks of the Yakokut graben are similar to the alkaline gabbroids and shonkinites of the Inagli massif. Based on the fact that the Yakokut differentiated picritoids contain about wt. 26% of the normative olivine (according to CIPW), it is shown that by calculating the complete separation of 25% of olivine from the composition of picritoids, we obtain a residual melt that is extremely close to the shonkinites of the the Yakokut graben and Inagli massif ‘Table 1’. The following calculation of the mixing of 75% of shonkinite and 25% of dunite of the Inagli produces a result almost indistinguishable from the average composition of K-picritoids of the Yakokut graben [4]. This overlap of the results on the recalculation of rocks from different remote areas shows a similar path of their crystallization differentiation. Therefore, it can be assumed that the Inagli massif was formed in the Early Cretaceous from high-potassium picrite magma. According to the model proposed by V.S. Shkodzinsky [10], at the latest stages of ascent, melts can be subjected to an abrupt decompression solidification and extraction in the form of a highly viscous magmatic diapir of cylindrical shape. Its apical and peripheral parts were composed primarily of shonkinites, whereas dunites are cumulate rocks formed in an extended cylindrical column confined to a weakened zone of fault intersection ‘Figure 1’.

Tab. 1. Calculated composition (wt.%) of the initial melt that formed the rocks of the Inagli massif

Rock and melts	n	SiO_2	TiO_2	Al_2O_3	Fe_2O_3	FeO	MnO	MgO	CaO	Na_2O	K_2O	P_2O_5
Picritoids[1] of the Yakokut graben	18	46.45	0.68	7.32	5.56	5.86	0.16	18.36	9.45	0.66	4.78	0.72
Porphyritic olivine[2] from picritoids	1	40.62	0.00	0.00	0.00	12.43	0.00	46.26	0.68	0.00	0.00	0.00
Residual melt = (1 × picritoids[1] – 0,25 × olivine[2])/0,75	–	48.39	0.90	9.76	7.42	3.67	0.21	9.05	12.37	0.88	6.37	0.96
Shonkinites[3] of the Yakokut graben	1	48.69	0.88	10.15	5.22	5.75	0.14	9.80	10.14	0.35	7.72	1.17
Inagli shonkinites[4]	27	49.95	0.93	9.71	5.18	5.06	0.17	9.28	10.87	1.74	5.95	1.17
Inagli dunites[5]	79	40.81	0.09	0.09	3.83	3.83	0.12	50.44	0.54	0.12	0.08	0.04
Initial melt for the Inagli massif = (0.75 × shonkinites[4] + 0.25 × dunites[5])	–	47.67	0.72	7.30	4.84	4.75	0.16	19.57	8.29	1.33	4.48	0.89

Note. n, Number of analyses; [1] average composition of differentiated picritoids of the Yakokut graben; [2] composition of porphyritic olivine from picritoids; [3] shonkinites of the Yakokut graben [9]; [4,5] rocks of the Inagli massif. Analytical results were recalculated to a 100% dry residue.

The Inagli massif is part of the alkaline rock association of the northern part of the Aldan shield, represented by volcanic and intrusive bodies of syenites, shonkinites, potassium lamprophyres, picrites, and others [11, 12]. It is assumed that the vast MZ area of igneous alkaline rocks ‘Figure 3’ located to the north of the South Aldan back-arc trough is part of the rear zone of the active continental margin and was formed as a result of subduction processes associated with the impact of the Mongol-Okhotsk belt on the southern margin of the Siberian craton [13]. Zonal massifs of the Ural-Alaskan type, according to many authors [e.g. 14, 15], are formed in the suprasubduction-island-arc setting of mobile regions and are therefore characterized by elongated forms along the strike of orogenic belts, often acquiring deformed outlines and inclined tectonic contacts. In contrast, the formation of the Aldan shield massifs was characterized by more stable conditions of the back-arc of the active continental margin, which determined the preservation of the primary zonal-annular and vertical diapyroid structure of the massifs [4].

The intrusion of the ore-magmatic systems from different levels of a long-term developing subduction zone to the surface is likely to occur under different conditions. This will lead to the formation of various genetic types of ores: from gold-platinoid ores associated with concentric-zonal intrusions to gold-copper-porphyry deposits with accompanying scarn, metasomatic, vein, stratoid and other ore occurrences. Zonation established on the Aldan shield is expressed in an increase of the potassium alkalinity of igneous rocks from south to north, so this type of zonation can be explained by marginal continental and island-arc settings, i.e. it is related to the Benioff zone [12]. Hence, the differences in mineralogy and geochemistry of platinum-bearing and gold-bearing bodies of different types are due to different depths of origin of the ore-magmatic systems, with their further evolution being similar to the formation model of intrusion-related gold system (IRGS) [e.g. 16, 17].

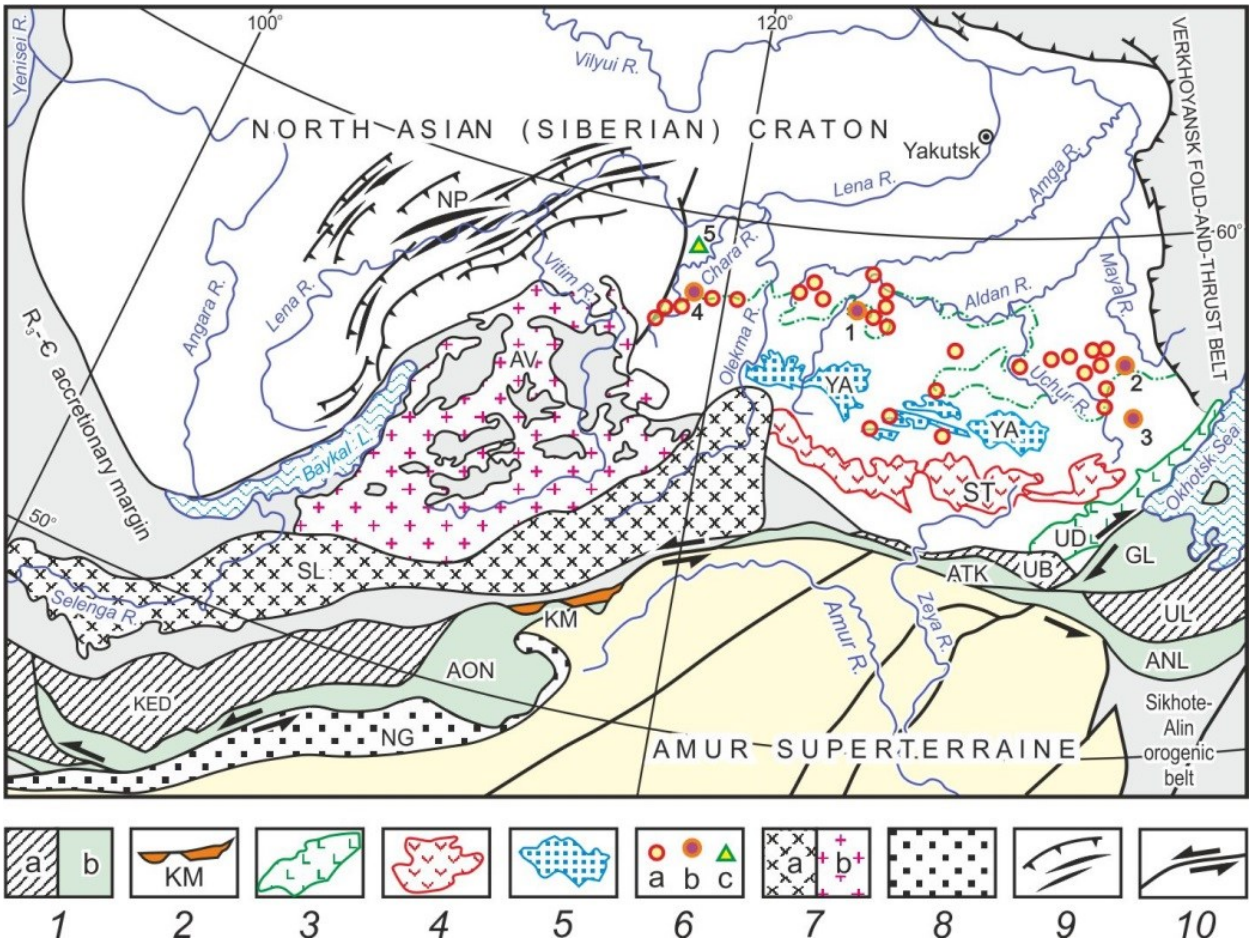

Fig. 3. Tectonic scheme of the southern margin of the North Asian (Siberian) craton modified after [13]. 1-2, terranes of the Mongol-Okhotsk orogenic belt: 1a – accretionary wedge terraines (KED - Khentei-Daursky, UB - Unya-Bomsky); 1b – oceanic rocks (AON - Ononsky, ATK - Tukuringsky, ANL - Nilansky, GL - Galamsky); 2, continental margin (KM - Kamensky). 3-8 – continental marginal magmatic arc associated with subduction zone of T_3-K_1 (3-6) and PZ-T_1 (7-8) ages: 3 – Udskoy (UD) volcanic-plutonic belt; 4 – Stanovoy (ST) plutonic belt; 5 – South Aldan (YA) depressions; 6 – alkaline magmatites: a - stocks and dikes, b - zonal ring intrusions: Inagli (1), Konder (2), Chad (3) and Murunsky complex (4); c - Molbo River dike (5); 7a – Selenginsky (SL) volcano-plutonic belt; 7b – Angara-Vitim (AV) giant granitoid batholith; 8 – North Gobi (NG) forearc basin; 9 – Nepskaya (NP) folds-and-thrusts zone; 10 – strike-slip and transform faults. The dashed-dot green line is the northern border of the Aldan Shield with a Rhiphean-Cambrian platform cover.

Oxygen Thermobarometry of the Inagli Massif Rocks

The characteristic of the redox state of magmatites possesses an essential significance for determining the conditions of the origin and evolution of ore-magmatic systems in association with their potential ore-generating capacity. The assessment of the redox state of the rocks of the Inagli massif was conducted by the author using the olivine-spinel oxygen thermobarometer BBG [3]:

$$T,(K) = \left[(6530 + 280P + 7000 + 108P)\left(1 - 2X_{Fe}^{ol}\right) - 1960\left(X_{Mg}^{sp} - X_{Fe^2}^{sp}\right) + 16150X_{Cr}^{sp} + 25150\left(X_{Fe^3}^{sp} + X_{Ti}^{sp}\right)\right]/(R * \ln K_D^{ol-sp} + 4.705)$$, where $K_D^{ol-sp} = (X_{Mg}^{ol} * X_{Fe2}^{sp})/(X_{Fe}^{ol} * X_{Mg}^{sp})$;

$$\Delta \lg(fO_2)^{FMQ} = 0.27 + 2505/T - 400P/T - 6\lg\left(X_{Fe}^{Ol}\right) - 3200\left(1 - X_{Fe}^{Ol}\right)^2/T + 2\lg\left(X_{Fe^{2+}}^{sp}\right) + 4\lg\left(X_{Fe^{3+}}^{sp}\right) + 2630(X_{Al}^{sp})^2/T$$, where T is in K, P in GPa, R is the gas constant, X_{Cr}^{sp}, $X_{Fe^3}^{sp}$, X_{Al}^{sp} the R^{3+}/total R^{3+} ratio in spinel, X_{Ti}^{sp} the number of Ti cations in spinel to 4 oxygens, and X_{Mg}^{ol}, and $X_{Fe^{2+}}^{sp}$ the $Fe^{2+}/(Fe^{2+} + Mg)$ ratios in olivine and spinel.

Some representative analyses of coexisting olivine-spinel associations from rocks and platinum-chromitite ore segregations are given in 'Table 2', and the results of calculations are shown in the diagram $lgfO_2$ – T 'Figure 4'.

Thus, the oxygen fugacity values for the coexisting olivine-chromespinel parageneses from dunites, peridotites, shonkinites, chromitites and olivine-chromite inclusions in the isoferroplatinum nuggets of the Inagli massif stretch along the trend FMG+(2-4), i.e. by (2-4) units of $lgfO_2$ exceeding the fayalite-magnetite-quartz (FMG) buffer, in the range 620-1140^{0}C. This rather narrow range of fluctuations in the values of O_2 fugacity in a wide temperature interval indicates favorable comparability and reliability of the obtained data. Inclusions of Cr-spinels in olivine from shonkinites, peridotites and dunites form similar trends ranging 710-840, 770-890 and 620-930^{0}C, respectively. Values of $lgfO_2$ for paragenetic Ol-Sp assemblage from chromitites and isoferroplatin nuggets continue this trend to even higher temperatures of 710-980 and 680-1140^{0}C, respectively. This confirms the model previously proposed by the author, which implies separation of a Cr-rich oxide liquid with significant concentration of the platinum-group elements from a mafic magma, as well as the formation of all rocks of the Inagli massif during the crystallization differentiation of picritoid magma. It is further notable that these values correspond to the field of values for dunites and chromitites of the Ural platinum-bearing belt obtained by other researchers [18] using the oxygen thermobarometer BBG.

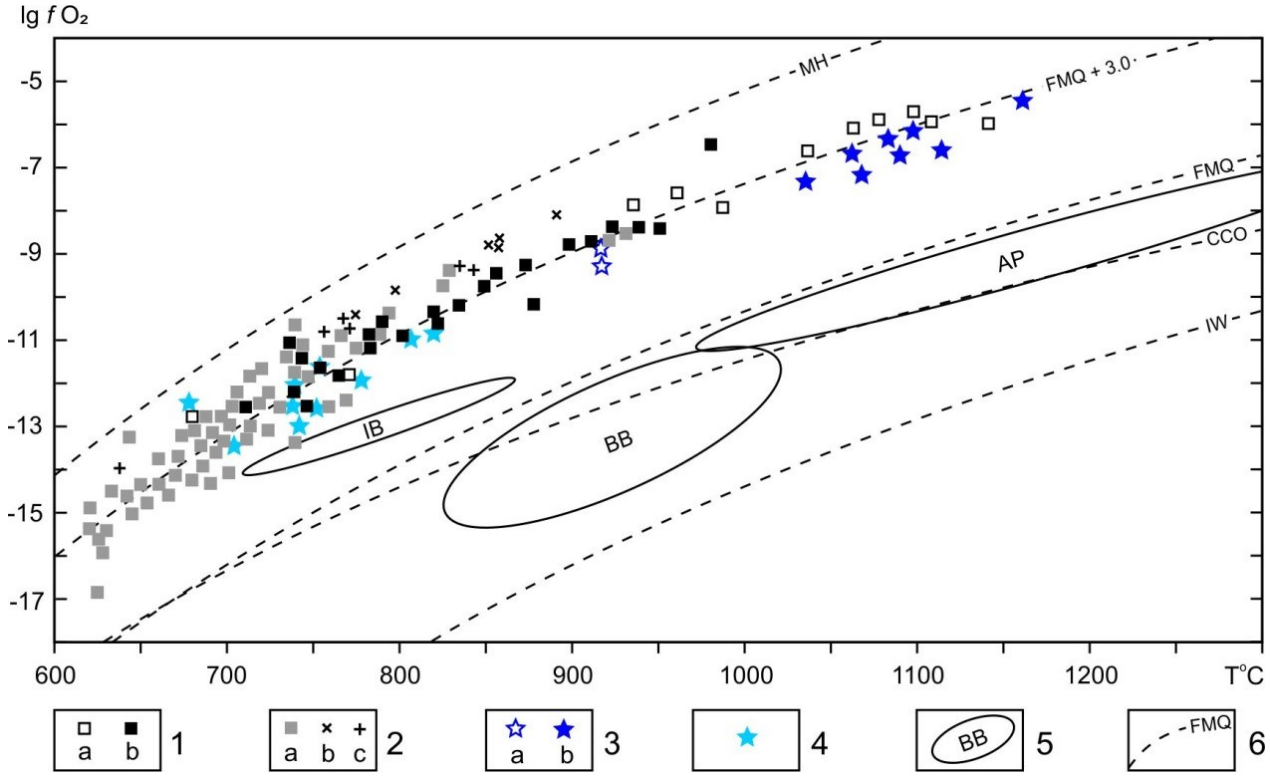

Fig. 4. $LogfO_2$ – T diagram calculated for olivine-spinel assemblages by oxygen thermobarometer BBG [3].
1, intergrowths with isoferroplatinum (a) and Cr-spinel (b) from the Inagli placer; 2, dunite (a), peridotite (b) and shonkinite (c) of the Inagli massif. 3-4, platinum-bearing massif of the Urals by [18]: dunite (a) and chromitite (b) of the Nizhnii Tagil massif; 4, dunite of the Kytlym massif; 5, fields after [18]: BB - peridotites of the Beni-Bushera massif [19]; AP – abyssal peridotite from the ocean ridge systems [20]; IB – peridotites from the Izu-Bonin-Mariana forearc [21]; 6 – oxygen buffer curves for magnetite-hematite (MN) [22], fayalite-magnetite-quartz (FMQ) [23], carbon-oxygen-CO (CCO) [24] and iron-wustite (IW) [23] calculated for pressures of 1 GPa.

Tab. 2. Representative analyses co-existing olivine (Fa $_{mol}$%) and spinel (wt. %) of the Inagli massif

No.	Fa	TiO_2	Al_2O_3	Cr_2O_3	Fe_2O_3	FeO	MnO	MgO	Total	Ti	Al	Cr	Fe^{3+}	Fe^{2+}	Mn	Mg
Dunites																
5-5	11	0.89	2.26	34.31	32.80	26.07	0.59	4.20	101.12	0.024	0.095	0.972	0.885	0.782	0.018	0.224
4-21	8	0.82	4.15	37.29	28.13	22.36	0.62	6.56	99.93	0.022	0.172	1.039	0.746	0.659	0.018	0.345
2-14	9	0.68	5.02	42.75	22.78	23.03	0.52	6.54	101.32	0.018	0.204	1.168	0.592	0.666	0.015	0.337
5-3	10	0.41	1.74	45.04	25.23	21.69	0.49	6.96	101.56	0.011	0.072	1.244	0.663	0.634	0.014	0.362
2-14	8	0.76	4.96	45.54	19.60	21.55	0.50	7.38	100.29	0.020	0.202	1.247	0.511	0.624	0.015	0.381
2-8	9	0.70	3.77	46.73	20.10	22.07	0.52	6.98	100.87	0.018	0.154	1.284	0.526	0.641	0.015	0.362
2-6	6	0.81	8.32	47.94	13.89	19.96	0.53	8.83	100.28	0.021	0.330	1.276	0.352	0.562	0.015	0.443
6-12	5	0.55	7.07	49.84	14.35	19.50	0.57	8.91	100.79	0.014	0.281	1.328	0.364	0.550	0.016	0.448
1-1	6	0.80	8.55	50.98	11.15	19.48	0.35	9.39	100.71	0.020	0.336	1.344	0.280	0.543	0.010	0.467
60	5	0.69	5.76	52.13	15.05	16.56	0.34	11.10	101.63	0.017	0.225	1.366	0.375	0.459	0.010	0.548
4-2	6	0.65	8.58	52.30	9.78	16.93	0.38	10.67	99.28	0.016	0.338	1.383	0.246	0.474	0.011	0.532
34	6	0.53	5.90	52.75	12.82	18.10	0.50	9.64	100.24	0.013	0.235	1.412	0.327	0.512	0.014	0.486
3-8	6	0.69	6.69	53.26	9.78	21.37	0.52	7.64	99.95	0.018	0.270	1.443	0.252	0.612	0.015	0.390
85	5	0.66	4.59	54.19	14.92	14.35	0.24	12.42	101.37	0.016	0.179	1.417	0.371	0.397	0.007	0.613
5-7	6	0.75	5.32	54.35	12.91	13.90	0.39	12.50	100.11	0.019	0.209	1.431	0.323	0.387	0.011	0.621
3-10	7	0.89	6.17	54.52	9.16	19.48	0.44	8.93	99.59	0.023	0.248	1.471	0.235	0.556	0.013	0.454
6-13	6	0.52	8.95	55.11	7.16	15.35	0.45	11.61	99.16	0.013	0.350	1.445	0.179	0.426	0.013	0.574
3-1	6	0.64	5.04	55.20	10.35	20.42	0.52	8.14	100.31	0.017	0.204	1.496	0.267	0.586	0.015	0.416
5-7	6	0.70	4.92	55.42	12.41	14.11	0.39	12.34	100.29	0.018	0.193	1.460	0.311	0.393	0.011	0.613
4-14	6	0.56	6.98	57.15	7.63	16.84	0.46	10.69	100.31	0.014	0.274	1.506	0.192	0.470	0.013	0.531
11-1	7	0.59	3.93	58.28	8.44	21.43	0.35	7.51	100.54	0.015	0.160	1.590	0.219	0.619	0.010	0.386
Chromitites																
50	6	0.76	4.37	48.12	22.47	13.46	0.26	13.21	102.66	0.019	0.168	1.243	0.552	0.368	0.007	0.643
1-10	6	0.82	6.30	52.63	13.11	16.66	0.42	10.99	100.93	0.021	0.247	1.384	0.328	0.463	0.012	0.545
43-1	6	0.90	5.88	54.64	10.80	18.19	0.25	10.09	100.75	0.023	0.233	1.450	0.273	0.511	0.007	0.505
5-7	8	0.68	6.38	55.02	10.60	16.67	0.38	10.90	100.63	0.017	0.251	1.450	0.266	0.464	0.011	0.542
4-1	7	0.70	4.96	55.37	12.88	14.94	0.33	12.02	101.21	0.017	0.194	1.450	0.321	0.414	0.009	0.594
20	6	0.74	5.89	56.18	11.88	13.23	0.26	13.39	101.58	0.018	0.226	1.447	0.291	0.360	0.007	0.650
285	6	0.59	5.85	57.45	8.43	17.44	0.33	10.29	100.39	0.015	0.232	1.526	0.213	0.490	0.009	0.515
Isoferroplatinum nuggets																
9	5	0.70	5.08	54.58	13.23	11.80	0.41	13.66	99.46	0.017	0.199	1.435	0.331	0.328	0.012	0.677
5	5	0.74	5.96	54.95	12.63	10.27	0.37	14.88	99.79	0.018	0.230	1.423	0.311	0.281	0.010	0.727
44	5	0.70	5.90	56.41	8.50	15.63	0.62	11.01	98.77	0.018	0.236	1.512	0.217	0.443	0.018	0.557
14	5	0.68	6.86	58.60	8.80	10.55	0.51	14.94	100.93	0.016	0.261	1.493	0.213	0.284	0.014	0.718
16	5	0.63	6.64	58.97	9.11	8.56	0.51	16.09	100.51	0.015	0.251	1.498	0.220	0.230	0.014	0.771
Peridotite (63) and shonkinites (4-18. 4-19)																
63	24	7.47	2.18	1.00	53.14	35.11	0.31	2.06	101.26	0.203	0.093	0.028	1.473	1.082	0.010	0.111
4-18	26	7.25	2.20	0.81	53.46	35.41	0.33	1.84	101.31	0.201	0.095	0.024	1.480	1.089	0.010	0.101
4-19	28	6.46	2.46	0.68	53.06	34.67	0.32	1.43	99.08	0.183	0.109	0.020	1.504	1.093	0.010	0.080

Note: Composition of minerals were carried out on a Camebax-Micro microprobe analyzer. the contents of Fe_2O_3 and FeO are determined by recalculation according to the stoichiometric spinel formula.

Conclusion

In terms of redox parameters. platinum-bearing zonal ultramafic-mafic massifs of the Ural-Alaskan and Aldanian types are close to more oxidized peridotites with a long histories in the lithosphere or from subduction zones [25]. for example. peridotites of the supra-subduction zones of the Izu-Bonin-Mariana fore-arc. They differ significantly from the subcontinental peridotites of the Beni-Bushera massif. as well as abyssal peridotites of oceanic ridge systems formed at the more reduced conditions in the range between FMQ. CCO and IW buffers. i.e. in the stability zone of graphite and diamond. Judging by the olivine-spinel equilibrium. the formation of rocks in the Inagli massif began at temperatures above 1140°C. when the appearance of early magmatic ore platinum-chromitite segregations is recorded. The abundant joint crystallization of olivine and accessory chromespinel in dunites is noted below 930°C and continues up to 620°C.

The mineralogical and geochemical characteristics of the rocks and geological and morphological specifics of the intrusion show that the initial massif-forming melt was of high-K picritoud composition. Reaching the subsurface levels. it underwent a gradual decompression solidification and further upward movement of viscous magma in the form of a cylindrical diaper-like

body. The supply of new portions of various differentiates from the lower horizons of the magma column caused a complex concentric-zonal structure of the Inagli massif.

Acknowledgments

The author thanks all colleagues who participated in analytical and laboratory work. This study was carried out within the State Assignment for Diamond and Precious Metal Geology Institute SB RAS.

References

1. 1. I.S. Rozhkov. V.I. Kitsul. L.V. Razin. S.S. Borishanskaya. Platinum of the Aldan Shield (Publishing House of Academy of Sciences USSR. Moscow. 1962).
2. A.M. Korchagin. The Inagli Pluton and Its Mineral Resources (Nedra. Moscow. 1996).
3. C. Ballhaus. R.F. Berry. D.H. Green. "High pressure experimental calibration of the olivine-orthopyroxene-spinel oxygen geobarometer: implication for the oxidation state of the upper mantle". Contributions to Mineralogy and Petrology 107. 27–40 (1991).
4. A.V. Okrugin. A.S. Borisenko. A.I. Zhuravlev. A.V. Travin. "Mineralogical. geochemical. and age characteristics of the rocks of the Inagli dunite–clinopyroxenite–shonkinite massif with platinum–chromite and Cr-diopside mineralization (Aldan Shield)". Russian Geology and Geophysics 59. 1301–1317 (2018).
5. A.V. Okrugin. "Crystallization–liquation model of formation of PGE–chromite ores in mafic–ultramafic complexes". Tikhookeanskaya Geologiya 23. 63–75 (2004).
6. G.I. Khudyakov. A.P. Kulakov. B.V. Ezhov. Morphotectonic CentralType Systems in Siberia and the Far East (Nauka. Moscow. 1988).
7. O. Yakubovich. A. Mochalov. A. Kotov. S. Sluzhenikin. A. Okrugin. M. Daniík. B. McDonald. N. Evans. B. Mclnnes. "190Pt–4He dating of platinum mineralization." in: Mineral Resources in a Sustainable World. Proc. 13th SGA Biennial Meet.. 24–27 August 2015. (Nancy. France. 2015) pp. 663–664.
8. A. Okrugin. A. Zhuravlev. O. Yakubovich. "Geodinamic setting for formation of the mesozoic au-pt deposits of the Aldan shield." in Geology and mineral resources of the North-East of Russia: materials of the X All-Russian Scientific and practical conference. (NEFU Publishing House. Yakutsk. 2020) pp. 266-272.
9. A.P. Krivenko. "Mesozoic Potassic Picritoids of Central Aldan". Doklady Akad. Nauk SSSR 254. 465–467 (1980).
10. V.S. Shkodzinskii. Global Petrology according to Modern Data on the Hot Heterogeneous Accretion of the Earth (Publishing House of SVFU. Yakutsk. 2018).
11. A.Ya. Kochetkov. "Mesozoic gold-bearing ore magmatic systems of Central Aldan". Russian Geology and Geophysics 47. 850-864 (2006).
12. E.P. Maximov. V.I. Uyutov. V.M. Nikitin. "The Central Aldan gold-uranium ore magmatogenic system (Aldan-Stanovoy shield. Russia)". Tikhookeanskaya Geologiya 29. 3–26 (2010).
13. L.M. Parfenov. L.I. Popeko. O. Tomurtogoo. "Problems of the tectonics of the Mongol–Okhotsk orogenic belt". Tikhookeanskaya Geologiya 19. 24–43 (1999).
14. R.G. Yazeva. V.V. Bochkarev. "Ural platinum-bearing belt and Tagil paleoarc: magmatism and geodynamie relations". Geotectonics. No. 2. 75-86 (2003).
15. V.R. Shmelev. "Magmatic complexes of a Main Urals fault zone (Prepolar sector) in light of new geochemical datas". Litosfera. No. 2. 41-59 (2005).
16. J.R. Lang and T. Baker. "Intrusion-related gold systems: the present level of understanding". Mineralium Deposita 36. 477-489 (2001).
17. M. Economou-Eliopoulos. "PGE potential of porphyry deposits". in Exploration for deposits of platinum-group elements. (Mineral. Association of Canada Short Course 35. Oulu. 2005). pp. 203-245.
18. I.S. Chashukhin. S.L. Votyakov. E.V.Pushkarev et al.. "Oxythermobarometry of ultramafic platinum-bearing belt of the Urals". Geochemistry No. 8. 846–863 (2002).
19. A. Woodland. J. Kornprobst. B. Wood. "Oxygen thermobarometry of orogenic lherzolite massifs". Journal of Petrology 33. 203-230 (1992).
20. L.T. Brindzia. B.J. Wood. "Oxygen thermobarometry of abyssal spinel peridotites: the redox state and C–O–H volatile composition of the Earth's sub-oceanic upper mantle". Am. J. Sci. 290. 1093-1116 (1990).
21. R I.J. Parkinson and J.A. Pearce. "Peridotites from the Izu–Bonin–Mariana Forearc (ODP Leg 125): Evidence for Mantle Melting and Melt–Mantle Interaction in a Supra-Subduction Zone Setting". Journal of Petrology 39. 1577–1618 (1998).
22. R.G. Schwab. D. Küstner. "Die Gleichgewichtsfugazitaten technologisch und petrologisch wichtiger Sauerstoffpuffer". Neues Jahrb Mineral Abh. 140. 111-142 (1981).

References

23. H.St.C. O'Neill. "The quartz-fayalite-iron and quartz-fayalite-magnetite equilibria and the free energies of formation of fayalite (Fe2SiO4) and magnetite (Fe3O4)". Am. Mineral. 72. 67-75 (1987).
24. S. Jakobsson. N. Oskarsson. "The system C-O in equilibrium with graphite at high pressure and temperature: an experimental study". Geochimica et Cosmochimica Acta 58. 9-17 (1994).
25. D.J. Frost. C.A. McCammon. "The redox state of Earth's mantle". Annu. Rev. Earth Planet. Sci. 36. 389-420 (2008)